Design Study of a Converter Interface Interconnecting Energy Storage With the DC Link of a StatCom

Hailian Xie, Lennart Ängquist, *Member, IEEE*, and Hans-Peter Nee, *Senior Member, IEEE*

***Abstract*—Voltage-source converters (VSC) have been widely utilized to provide instantaneous reactive power support to power systems, an application referred to as static synchronous compensator (StatCom). The integration of energy storage (ES) into a StatCom makes it possible for the StatCom to provide a certain amount of active power as well as reactive power support. The possible benefit of the additional active power of a StatCom can be power oscillation damping capability, mitigation of phase-jump-related disturbances, etc. Direct connection of an ES device to the dc link of the VSC incurs an unnecessarily high-voltage rating of the VSC due to the considerable voltage swing associated with the ES device. Dual thyristor converter topology has been proposed as the interface between the ES and the dc link of the VSC. In this paper, a cost estimation for systems with the proposed interface topology is presented regarding three types of ES: capacitors, supercapacitors, and batteries. The study shows potential cost savings with utilization of the proposed interface topology. In addition, a cost comparison between different types of ES is presented, providing a guideline for the choice of ES in these kinds of applications.**

***Index Terms*—Cost estimation, dc link, dual thyristor converter, energy storage (ES), interface, StatCom, static synchronous compensator, voltage-source converters (VSCs).**

NOMENCLATURE

CST_{T_1}	Cost of transformer T1.
CST_{T_2}	Cost of transformer T2.
C_{ES}	Capacitance of ES capacitor.
C_{SC}	Capacitance of supercapacitor banks.
C_{1_SC}	Capacitance of a single cell supercapacitor.
$E_{\mathrm{base,C}}$	Capacitor energy base.
$E_{\mathrm{base,SC}}$	Supercapacitor energy base.
I_{base}	Base current.
P_{ES}	Active power privided by ES.
P_R	Average power loss of the supercapacitor.
P_{Rs}	Average power loss of the supercapacitor during a subperiod.
P_{thy}	Power from the dual thyristor converter.
$P_{\mathrm{thy,max}}$	Maximum power from the thyristor converter.
R_{ES}	Resistance of the supercapacitor banks.
$S_{\mathrm{Vw}}, S_{\mathrm{Vw}}$	VSC power rating with and without the interface.
S_{base}	Base power.
S_{thy}	Power rating of the dual thyristor converter.
U_b	RMS value of the line-to-line bus voltage.
U_{base}	Base voltage.
$U_{\mathrm{d,min}}$	Minimum dc-side voltage.
U_v	Magnitude of the VSC output ac voltage.
cst_C	Cost of a 100-MJ dc capacitor.
cst_V	Cost of a 100-MVA VSC.
$\mathrm{cst}_{\mathrm{SC}}$	Cost of a 1000-MJ supercapacitor.
cst_{btr}	Cost of a 14400-MJ battery.
$\mathrm{cst}_{\mathrm{thy}}$	Cost of a 100-MVA dual thyristor converter.
$c_{\mathrm{ESw}}, c_{\mathrm{ESwo}}$	ES cost with and without the interface.
$c_{\mathrm{Vw}}, c_{\mathrm{Vwo}}$	VSC cost with and without the interface.
c_{thy}	Cost of the dual thyristor converter.
$c_{\mathrm{w}}, c_{\mathrm{wo}}$	Total system cost with and without the interface.
i_{C_2}	Current through capacitor C_2.
i_{ES}	Current from ES.
$i_{\mathrm{ES1}}, i_{\mathrm{ES2}}$	Current from the supercapacitor at the start and end instant of the first subperiod.
$i_{\mathrm{ES,f-1}}, i_{\mathrm{ES,f}}$	Current from the supercapacitor at the start and end instant of the last subperiod.
i_{thyd}	DC-side current of the thyristor converter.
$t_{P_{\mathrm{ES}}}$	ES discharge duration.
u_{ES}	ES terminal voltage.
$u_{\mathrm{ES1}}, u_{\mathrm{ES2}}$	Supercapacitor terminal voltage at the start and end instant of the first subperiod.

Manuscript received January 15, 2011; revised May 11, 2011; accepted June 20, 2011. Date of publication August 30, 2011; date of current version October 07, 2011. This work was supported by the ELEKTRA Research Program, which is administered by ELFORSK AB, Stockholm, Sweden. Paper no. TPWRD-00036-2011.

H. Xie is with ABB (China) Ltd.-Corporate Research, Beijing 100015, China (e-mail: hailian.xie@cn.abb.com).

L. Ängquist and H.-P. Nee are with the Royal Institute of Technology, Stockholm SE-100 44, Sweden (e-mail: lennart.angquist@ee.kth.se; hansi@kth.se).

Digital Object Identifier 10.1109/TPWRD.2011.2161677

$u_{\mathrm{ES,f-1}}, u_{\mathrm{ES,f}}$	Supercapacitor terminal voltage at the start and end instant of the last subperiod.
$u_{\mathrm{ES,min}}$	Minimum voltage of ES.
u_{N_SC}	Voltage of the supercapacitor banks.
u_{N1_SC}	Nominal voltage of a single-cell supercapacitor.
u_{SC}	Supercapacitor internal voltage.
$u_{\mathrm{SC1}}, u_{\mathrm{SC2}}$	Supercapacitor internal voltage at the start and end instant of the first subperiod.
$u_{\mathrm{SC,f-1}}, u_{\mathrm{SC,f}}$	Supercapacitor internal voltage at the start and end instant of the last subperiod.
$u_{\mathrm{SC,max}}$	Max. internal voltage of the supercapacitor.
u_{b_N}	Battery nominal voltage.
u_{b_chg}	Battery charging voltage.
u_{b_f}	Battery final discharging voltage.
$u_{b\_f\_\mathrm{w}}$	Battery final discharging voltage with interface.
u_d	VSC dc-side voltage.
x_v, x_{vn}	Phase reactor reactance in ohms and per unit.

I. Introduction

VOLTAGE-SOURCE converters (VSCs) are widely used for reactive power compensation, an application referred to as static synchronous compensator (StatCom). In the future, Smart Grid StatComs will probably become one of the most important components for flexible control of power systems on the transmission level and in distribution systems. By adding energy storage (ES) to a StatCom, the converter can provide a certain amount of active power (for instance, 20%) with a small reduction in the reactive power supply due to the quadratic relation between the active and reactive power. With the addition of active power support to the grid, different forms of energy management are enabled. It has also been reported that power oscillation damping [1]–[5] and power quality (PQ) and system stability improvement [6]–[11] can be achieved with the additional active power support of a StatCom. It has also been shown that a StatCom with active power compensation can mitigate disturbances, regarding phase jumps and magnitude fluctuations, created by sudden load changes in the connected network [12]. The additional capabilities obtained by adding active power support may, therefore, *significantly increase the security of the power supply*. Two cases where this might be particularly important are when weak grids are subjected to power variations from distributed energy sources and for outage management.

In this investigation, capacitors, supercapacitors (also known as ultracapacitors or electrochemical capacitors), and batteries are considered for ES. All three types of ES exhibit significant variations in the terminal voltage depending on the state of charge and on the magnitude and direction of the current. For instance, the variation of the terminal voltage for Ni-Cd batteries may be as high as 50% [13]. It, therefore, makes sense to consider an intermediate conversion stage between the ES and the dc link of the VSC, especially if the rated active power of the converter is only a fraction of the rated reactive power. If the dc-link voltage can be kept constant, substantial cost savings can be made since the voltage rating of the VSC does not have to be increased by adding the ES.

Topologies for interfacing ES with the dc link of a converter have been reported in the literature. They are for low- and medium-voltage applications and are mainly insulated-gate bipolar transistor (IGBT)-based bidirectional dc/dc converters either with a single leg [14], [15] or with three legs [16], [17]. Bidirectional dc/dc converters are commonly used as the interface between an ES device and the dc link of a converter in automotive power systems [18]–[21]. A three-port converter is proposed as the interface between the ES devices and the dc link of the single-phase converter in a single-phase line-interactive uninterruptible power-supply (UPS) system [22].

The cost of the additional conversion stage is, however, not insignificant even though this converter only has to have a rating corresponding to the rated active power of the VSC. An innovative way to reduce the rating of this converter is to have a converter which acts only on the difference in voltage between the ES and the dc link of the VSC. The rating of such a converter would be substantially lower than the rated active power of the VSC, and typically approximately one order of magnitude lower than the total rating of the VSC. In order to reduce the additional cost even more, thyristor-based technology may be chosen. This converter has been considered in this paper. The main properties of the converter have been described in [23] and [24].

Having the freedom to let the voltage of the ES vary without affecting the voltage rating of the VSC, the question is which kind of ES to use, and what potential cost savings can be obtained compared to the case without an interface between the ES and the dc link of the VSC.

Section II describes the foundations of the investigation. The method for cost estimation is presented in Section III. In Section IV, the total system cost is investigated with and without the converter interface between the ES and the dc link of the VSC. For each of the three types of ES, a cost comparison is made between the cases with and without the thyristor converter interface. A fixed energy-delivery period is considered. In Section V, the total system cost is again investigated using the three different types of ES. Different discharging/charging cycles have been considered and the costs using different types of ES are compared. The choice of the type of ES depends mainly on the amount of energy which is required during a typical discharging/charging cycle. In some cases, when several alternatives exist, the choice of the energy source must be made based on cost estimation.

In addition to capacitors, supercapacitors, and batteries, superconducting magnetic ES (SMES) is also considered in the literature as the ES to be integrated into a StatCom (e.g., in [4]). However, this paper discusses the cost of a proposed interface system between an ES and a VSC. Specifically, the study target is to obtain the relative cost with and without the interface using

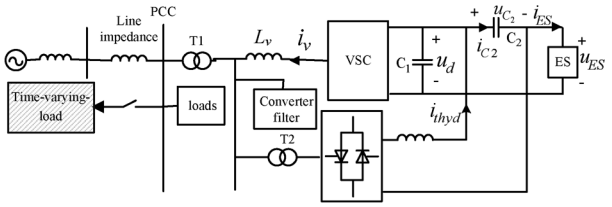

Fig. 1. Proposed dual converter interface for the ES devices.

TABLE I
RELATIVE COST OF DIFFERENT PARTS

Part	Symbol	Cost
Transformer T1(below 220 kV)	CST_{T_1}	0.5 pu
Transformer T2	CST_{T_2}	0.1 pu
VSC (100 MVA) with dc capacitor and phase inductor	cst_V	1 pu/100 MVA
Dual thyristor converter with dc inductor (VSC power)	cst_{thy}	0.5 pu/100 MVA
DC capacitor energy storage (VSC power during 1s)	cst_C	3.7 pu/100 MJ
Supercapacitor (VSC power during 10s)	cst_{SC}	1.1 pu/1000 MJ
Battery (4% of VSC power during 1h)	cst_{btr}	1.8 pu/14400 MJ

different ES devices. Since this paper is not a general comparison between costs of different ES systems and the information about the costs regarding SMES or other alternative systems (pumped hydro, compressed air ES or other) is difficult to access, only capacitors, supercapacitors, and batteries are considered in this paper.

II. FOUNDATIONS OF THE INVESTIGATION

A. Dual Thyristor Converter Interface

The dual thyristor converter interface topology is depicted in Fig. 1. The VSC is connected to the point of common coupling (PCC) via phase reactors and transformer T1. The VSC is supposed to deliver a certain amount of active power occasionally or periodically to the time-varying load at the PCC. The dual thyristor converter, consisting of two standard three-phase bridges, is fed through transformer T2 from the low-voltage side of transformer T1. The capacitor (C_2) on dc side of the thyristor converter is connected in series with the ES device and the whole branch is then connected in parallel with the dc-side capacitor (C_1) of the VSC. The antiparallel connection of the two thyristor bridges enables a 4-quadrant operation of the dual thyristor converter in the current-voltage plane. The output voltage of the thyristor converter is controlled so that the VSC dc voltage is always kept constant.

B. System Specifications and Comparison Method

The cost will be estimated relative to the cost of a 100-MVA VSC including the dc capacitor and the phase inductors. The relative costs of the different parts in the apparatus are listed in Table I.

The cost for the two transformers can be assumed to be constant for all cases. However, the costs of the ES, the VSC, and the thyristor converter vary from case to case and are proportional to the energy/power ratings.

The power flow during a discharging process has the following pattern. When a power P_{ES} is delivered from the ES device, the current passes through the thyristor converter. In addition, if the terminal voltage of the ES drops, the thyristor converter has to charge capacitor C_2 to keep the dc link voltage of the VSC. This requires a certain active power output from the thyristor converter. This power is provided by the VSC and is circulating through the VSC and the thyristor converter. The circulating power causes a further reduction in the reactive power support capability of the VSC. Therefore, a fair comparison should be the comparison of the total cost required for a certain amount of energy delivery in addition to the original reactive power support.

In the system shown in Fig. 1, the StatCom is supposed to provide a certain amount of active power P_{ES} for a certain duration $t_{P_{\mathrm{ES}}}$ in addition to the reactive power support. An active power support of 20% of the nominal apparent power will be considered in this study, which corresponds to a reduction of approximately 2% in the reactive power supply.

In the comparison in Section IV, the energy delivery periods for capacitors, supercapacitors, and batteries are set to 0.5 s, 30 s, and 15 min, respectively, based on the following consideration. Compared to supercapacitors, conventional capacitors have much lower capacitance and higher cost per energy unit. On the other hand, supercapacitors have a higher equivalent series resistance (ESR) [25], which means low efficiency at fast charging/discharging. Therefore, conventional capacitors are suitable for power delivery with short durations, whereas supercapacitors can only reach a reasonably high efficiency when they are charged and discharged in at least tens of seconds. Batteries also have certain internal resistance, which limits the charging/discharging efficiency. However, the cost per energy unit is much lower than that of capacitors and supercapacitors. This makes them suitable for long-period energy delivery (from minutes to hours).

The specifications of the system parameters are listed in Table II. The VSC phase reactors are 0.15 p.u. From the view point of converter voltage utilization, the phase reactors should be chosen as small as possible. However, the phase reactors are also used as a part of the converter filter circuit. A reduction of the phase reactor inductance, therefore, results in a higher current ripple. Based on the overall consideration of the aforementioned factors, a moderate value of 0.15 p.u. is chosen.

The minimum dc-side voltage level is calculated for the most demanding situation in which the converter is required to deliver the rated reactive power to keep the bus voltage at the nominal value. Hence, the magnitude (line-to-line, rms) of the converter output ac voltage should be

$$U_v = U_b + I_{\mathrm{base}} x_v = (1 + x_{vn}) U_{\mathrm{base}} \tag{1}$$

where $U_b = U_{\mathrm{base}}$ is the rms value of the line-to-line voltage at the bus, and x_{vn} is the phase reactor reactance in per unit.

TABLE II
SPECIFICATIONS OF THE SYSTEM PARAMETERS

VSC Rated power S_{base}	100 MVA	
VSC Rated current I_{base}	1.5 kA (RMS)	
Rated ac voltage U_{base}	38.5 kV (line-line, RMS)	
Phase reactor inductance x_{vn}	0.15 pu	
Active power to be delivered P_{ES}	20 MW (20% of the apparent power)	
Active power delivery duration $t_{P_{ES}}$	Capacitors	0.5 s
	Supercapacitors	30 s
	Batteries	15 min.

If sinusoidal PWM with third harmonic injection is utilized, the minimum dc side voltage is determined by

$$U_{d,\min} = \sqrt{2}(1 + x_{vn})U_{\text{base}}. \tag{2}$$

III. METHOD OF COST ESTIMATION

The total cost without the interface consists of three parts: 1) the cost of transformer T1, 2) the cost of the VSC, and 3) the cost of the ES devices, i.e.,

$$c_{\text{wo}} = c_{\text{ESwo}} + c_{\text{Vwo}} + \text{CST}_{T_1}. \tag{3}$$

The rating of the VSC has to be increased in proportion to the increase of the dc-side voltage, and so does the cost

$$c_{Vwo} = cst_V * u_{ES,\max}/U_{d,\min} \tag{4}$$

where $u_{ES\_\max}$ is the highest voltage of the ES.

Introduction of the proposed dual thyristor converter interface incurs two additional parts of cost: the cost of the dual thyristor converter and the cost of the thyristor converter transformer T2. The total cost, including the interface, is therefore given by

$$c_{\text{w}} = c_{\text{ESw}} + c_{\text{thy}} + c_{Vw} + \text{CST}_{T_1} + \text{CST}_{T_2}. \tag{5}$$

The rating of the VSC and the thyristor converter can be estimated as follows.

In the case of the thyristor converter interface, the VSC dc-side voltage is supposed to be kept constant at the minimum required value, i.e., $u_d = U_{d,\min}$.

The current from the ES is determined by the delivered power and the terminal voltage of the ES. Thus

$$i_{\text{ES}} = -P_{\text{ES}}/u_{\text{ES}}. \tag{6}$$

The current required to charge capacitor C_2 has to match the rate of change of u_{ES}. Accordingly

$$i_{C_2} = C_2\frac{d(u_d - u_{\text{ES}})}{dt} = -C_2\frac{du_{\text{ES}}}{dt}. \tag{7}$$

Therefore, the dc-side current of the thyristor converter is given by

$$i_{\text{thyd}} = i_{C_2} - i_{\text{ES}} = -C_2\frac{du_{\text{ES}}}{dt} + \frac{P_{\text{ES}}}{u_{\text{ES}}}. \tag{8}$$

The instantaneous power provided by the thyristor converter can now be expressed as

$$P_{\text{thy}} = (u_d - u_{\text{ES}})i_{\text{thyd}}. \tag{9}$$

The power rating of the thyristor converter is basically determined by the maximum active power delivery by the converter since the converter should be designed so that the power factor is close to unity when the active power reaches its maximum. Hence, the rating of the thyristor converter is given by

$$S_{\text{thy}} = P_{\text{thy, max}}. \tag{10}$$

Since the power provided by the thyristor converter will be circulating through the VSC and the thyristor converter, the VSC has to provide the circulating power and the power from the ES. Accordingly

$$P_{V,\max} = P_{\text{thy,max}} + P_{\text{ES}}. \tag{11}$$

The required power rating of the VSC, including the additional active power support, is now obtained as

$$S_{Vw} = \sqrt{S_{\text{base}}^2 + P_{V,\max}^2}. \tag{12}$$

The costs of the dual thyristor converter and the VSC can be estimated as

$$\begin{aligned} c_{\text{thy}} &= S_{\text{thy}} * cst_{\text{thy}}/S_{\text{base}} \\ c_{Vw} &= S_{Vw} * cst_V/S_{\text{base}} \end{aligned} \tag{13}$$

where cst_{thy} and cst_V are as given in Table I.

A. Capacitors as ES

1) With the Thyristor Converter Interface: With capacitors as the ES, (9) can be rewritten as

$$P_{\text{thy}} = \left(\frac{u_d}{u_{\text{ES}}} - 1\right)\left(\frac{C_2}{C_{\text{ES}}} + 1\right)P_{\text{ES}}. \tag{14}$$

For a certain power P_{ES} with a delivery period $t_{P_{\text{ES}}}$ and a certain ES capacitance C_{ES}, the minimum ES voltage is determined by

$$u_{\text{ES,min}} = \sqrt{U_{d,\min}^2 - 2P_{\text{ES}}t_{P_{\text{ES}}}/C_{\text{ES}}}. \tag{15}$$

The maximum power $P_{\text{thy, max}}$ delivered through the thyristor converter is then determined by the minimum ES voltage

$$P_{\text{thy, max}} = \left(\frac{u_d}{u_{\text{ES, min}}} - 1\right)\left(\frac{C_2}{C_{\text{ES}}} + 1\right)P_{\text{ES}}. \tag{16}$$

The costs of the VSC and the thyristor converter can then be estimated from (10)–(13).

The cost of the ES capacitor can be calculated as

$$c_{\text{ESw}} = \frac{1}{2}C_{\text{ES}}U_{d,\min}^2 * cst_C/E_{\text{base\_}C} \tag{17}$$

where $E_{\text{base\_}C} = 100$ MJ is the energy base for the capacitors, and cst_C is as given in Table I.

TABLE III
MAIN PROPERTIES OF DIFFERENT TYPES OF SUPERCAPACITORS

Technology type	Electrode materials	Energy storage mechanisms	Cell voltage	Energy density (Wh/kg)	Power density (kW/kg)
EDLC	Activated carbon	Charge separation	2.5-3	5-7	1-3
Pseudo-capacitors	Metal oxides Redox	charge transfer	2-3.5	10-15	1-2
Asymmetric capacitors	Carbon/ metal oxide	Double-layer/ charge transfer	2-3.3	10-15	1-2

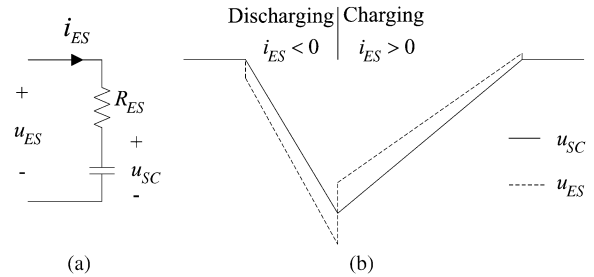

Fig. 2. (a) Representation of a supercapacitor. (b) Supercapacitor terminal voltage (dashed) and internal capacitor voltage (solid) during a discharging/charging cycle.

Finally, the total cost with the thyristor converter interface can be obtained with (5).

2) With Direct Connection: The cost of the VSC can be calculated from (4), with $u_{\mathrm{ES,max}}$ given by

$$u_{\mathrm{ES,max}} = \sqrt{U_{d,\min}^2 + 2P_{\mathrm{ES}}t_{P_{\mathrm{ES}}}/C_{\mathrm{ES}}} \tag{18}$$

and the cost of the ES can be estimated as

$$c_{\mathrm{ESwo}} = \frac{1}{2}C_{\mathrm{ES}}u_{\mathrm{ES,\,max}}^2 * cst_C/E_{\mathrm{base\_}C}. \tag{19}$$

Finally, the total cost is obtained from (3).

B. Supercapacitors as ES

There are three categories of supercapacitors: 1) electrochemical double layer capacitors (EDLC); 2) pseudocapacitors (also called pseudocapacitance supercapacitors); and 3) asymmetric capacitors (also called hybrid capacitors). Table III gives a comparison of their main properties [26]. Among the three types, EDLC is the most developed type. Since the majority of commercially available supercapaitors is EDLC [27], the information regarding supercapacitors in this paper refers to the EDLC type.

Supercapacitors have a much larger capacitance per cell than conventional capacitors. However, the ESR is also high. A supercapacitor can be represented by an internal capacitor and an ESR as shown in Fig. 2(a). Due to the ESR, the terminal voltage u_{ES} of the supercapacitor differs from the voltage u_{SC} across the internal capacitor during charging and discharging processes. These two voltages in a complete discharging/charging cycle are depicted in Fig. 2(b).

Commercially available single-cell supercapacitors have a maximum voltage rating of $u_{N1\_\mathrm{SC}} = 2.7$ V and the capacitance can be as high as $C_{1\_\mathrm{SC}} = 5000$ F. The dc ESR of a 2.7-V/5000-F supercapacitor cell can be 0.33 mΩ [28]. Single-cell supercapacitors can be connected in series to reach higher voltage ratings and in parallel to increase the capacitance. With M strings of supercapacitors having N series connected cells in each, the total capacitance, the voltage rating, and the total resistance are given by

$$\begin{aligned} C_{\mathrm{SC}} &= \frac{M}{N}C_{1\_\mathrm{SC}} \\ u_{N\_\mathrm{SC}} &= N * u_{N1\_\mathrm{SC}} \\ R_{\mathrm{ES}} &= \frac{C_{1\_\mathrm{SC}}}{C_{\mathrm{SC}}}\mathrm{ESR}. \end{aligned} \tag{20}$$

1) With Thyristor Converter Interface: Equation (16) can be used for estimation of the thyristor converter rating but with some modifications.

First, the term C_2/C_{ES} can be neglected since C_2 has a much lower value than the supercapacitor capacitance. This simplification yields

$$P_{\mathrm{thy,\,max}} = \left(\frac{u_d}{u_{\mathrm{ES,min}}} - 1\right)P_{\mathrm{ES}}. \tag{21}$$

Moreover, the power loss P_R in the ESR should be taken into consideration in the determination of $u_{\mathrm{ES,min}}$.

The power loss P_R varies with the drop of the supercapacitor voltage. To find out the average loss during the power delivery period, the whole period is divided into certain subperiods with equal durations. The power loss P_{Rs} during each subperiod can be approximated as the average of the losses at the start instant and the end instant of the subperiod and can be obtained as follows.

Start from the first subperiod. At the start instant, the internal voltage of the supercapacitor is $u_{\mathrm{SC1}} = U_{d,\min}$ and the current i_{ES1} into the ES is determined by

$$-(u_{\mathrm{SC1}} + i_{\mathrm{ES1}}R_{\mathrm{ES}})i_{\mathrm{ES1}} = P_{\mathrm{ES}}. \tag{22}$$

The current i_{ES2}, the internal voltage u_{SC2}, and the terminal voltage u_{ES2} of the supercapacitor at the end instant of the subperiod can be obtained together with P_R by numerically solving the equation set

$$\begin{aligned} P_{Rs} &= (P_{Rs1} + P_{Rs2})/2 \\ &= \left(i_{\mathrm{ES1}}^2 + i_{\mathrm{ES2}}^2\right)R_{\mathrm{ES}}/2 \\ u_{\mathrm{ES2}} &= u_{\mathrm{SC2}} + i_{\mathrm{ES2}}R_{\mathrm{ES}} \\ u_{\mathrm{ES2}}i_{\mathrm{ES2}} &= -P_{\mathrm{ES}} \\ (P_{\mathrm{ES}} + P_{\mathrm{Rs}})\Delta t &= C_{\mathrm{SC}}\left(u_{\mathrm{SC1}}^2 - u_{\mathrm{SC2}}^2\right)/2 \end{aligned} \tag{23}$$

where Δt is the time step.

For the following subperiods, the terminal voltage and the average loss can be obtained from (23) with i_{ES1} and u_{SC1} known from the end of the previous subperiod.

The mean value of all average losses in all subperiods gives the overall average loss P_R. The terminal voltage $u_{\mathrm{ES,min}}$ at the end instant of the whole discharging process is obtained from the calculation for the last subperiod.

With $P_{\text{thy, max}}$ given by (21), the costs of the VSC and the thyristor converter can then be estimated with (10)–(13).

The cost of the ES is calculated as

$$c_{\text{ESw}} = \frac{1}{2} C_{\text{SC}} U_{d,\min}^2 * cst_{\text{SC}} / E_{\text{base\_SC}} \tag{24}$$

where $E_{\text{base\_SC}} = 1000\,\text{MJ}$ is the energy base for supercapacitors.

Finally, the total cost with the thyristor converter interface is obtained from (5).

Since the recharging process after the energy delivery can always be controlled slower than the discharging process that is determined by the energy demand of the system, the rating calculations described here are based on the energy delivery process.

2) With Direct Connection: At the end instant of the discharging process, the terminal voltage, internal voltage, and the current of the supercapacitor are determined by

$$\begin{aligned} u_{\text{ES},f} &= U_{d,\min} \\ u_{\text{SC},f} &= u_{\text{ES},f} - i_{\text{ES},f} R_{\text{ES}} \\ i_{\text{ES,f}} &= -P_{\text{ES}} / u_{\text{ES,f}}. \end{aligned} \tag{25}$$

To determine the maximum voltage across the supercapacitor, the losses should be taken into account. Similar to the method utilized in the previous subsection, the whole energy delivery period is divided into equal subperiods. Calculations are made from the end instant to the start instant of the discharging period with certain time steps. For the first subperiod, the current $i_{\text{ES,f}-1}$, the terminal voltage $u_{\text{ES,f}-1}$ and the internal $u_{\text{SC,f}-1}$ at the start instant t_{f-1}, together with the average loss P_{Rs} in the subperiod, can be obtained by solving the equation set

$$\begin{aligned} P_{Rs} &= (P_{Rs,f} + P_{Rs,f-1})/2 \\ &= \left(i_{\text{ES,f}}^2 + i_{\text{ES,f}-1}^2\right) R_{\text{ES}}/2 \\ u_{\text{ES,f}-1} &= u_{\text{SC,f}-1} + i_{\text{ES,f}-1} R_{\text{ES}} \\ u_{\text{ES,f}-1} i_{\text{ES,f}-1} &= -P_{\text{ES}} \\ (P_{\text{ES}} + P_{Rs})\Delta t &= C_{\text{SC}} \left(u_{\text{SC,f}-1}^2 - u_{\text{SC,f}}^2\right)/2. \end{aligned} \tag{26}$$

The maximum ES voltage $u_{\text{ES, max}} = u_{\text{SC, max}}$ is then obtained from the calculation of the last subperiod.

The cost of the VSC can be calculated with (4). The cost of the ES can be estimated as

$$c_{\text{ESwo}} = \frac{1}{2} C_{\text{SC}} u_{\text{ES, max}}^2 * cst_{\text{SC}} / E_{\text{base\_SC}}. \tag{27}$$

Finally, the total cost can be obtained from (3).

C. Batteries as ES

The battery voltage does not drop as rapidly as the capacitor voltage during discharge. However, the final voltage can still be significantly lower than the nominal voltage. Due to the internal resistance, the charging voltage of a battery cell is higher than the nominal voltage. Table IV lists the cell voltages of several battery technologies: sodium/nickel chloride or zero-emission battery research activities (ZEBRA) batteries [29], sodium-sulfur (NaS) batteries [30], nickel-cadmium (Ni-Cd) batteries [13], lead-acid batteries [31], and lithium-ion (Li-ion) batteries [32]. As can be seen, the voltage swing of batteries (from the final discharging voltage to the charging voltage) can be as high as 65% (e.g., ZEBRA batteries).

TABLE IV
CELL VOLTAGE AND PRIMAY APPLICATIONS OF DIFFERENT BATTERIES

Battery type	Nominal voltage (V)	Final voltage (V)	Charging voltage (V)	Primary applications
ZEBRA	2.58	1.72	2.85	Vehicle, telecommunication, marine application
NaS	2.08	1.82	2.3	Bulk energy storage
Ni-Cd	1.2	1.0	1.5	Backup system, engine starting, stationary energy storage
Lead-Acid	1.94	1.79	2.3	Backup system, vehicle, stationary energy storage
Li-Ion	3.6	2.7	4.0	Portable electronics, vehicles, backup system

Let the nominal voltage of the ES battery be u_{b_N} and the charging voltage be u_{b_chg}. Assume that the charging voltage and the nominal voltage are $x\%$ and $y\%$ higher than the final discharging voltage u_{b_f} respectively, i.e.,

$$\begin{aligned} u_{b\_\text{chg}} &= (1 + x\%) u_{b\_f} \\ u_{b\_N} &= (1 + y\%) u_{b\_f}. \end{aligned} \tag{28}$$

1) With the Thyristor Converter Interface: The nominal voltage of the ES battery is designed to be the same as the dc-link voltage of the VSC in this case, i.e., $u_{b\_N} = u_d = U_{d,\min}$. Correspondingly, the final discharging voltage should be

$$u_{b\_f\_\text{w}} = U_{d,\min}/(1 + y\%). \tag{29}$$

Since the voltage changing rate of the battery is moderate and C_2 is small, the charging current given in (7) is much smaller than the ES current in (8) and can thus be neglected in the thyristor converter rating calculation

$$P_{\text{thy, max}} \approx \left(\frac{u_d}{u_{b\_f\_\text{w}}} - 1\right) P_{\text{ES}} = y\% P_{\text{ES}}. \tag{30}$$

The costs of the thyristor converter and the VSC are then determined by (10)–(13).

The cost of the battery is determined by the energy level almost independent on the voltage level. Hence, this cost will remain unchanged regardless of whether there is an interface or not and it is given by

$$c_{\text{ES}} = P_{\text{ES}} * t_{P_{\text{ES}}} * cst_{btr} / E_{\text{base\_}b} \tag{31}$$

where cst_{btr} is as given in Table I. P_{ES} and $t_{P_{\text{ES}}}$ are in megawatts and minutes, respectively.

Finally, the total cost with the thyristor converter interface can be obtained from (5).

2) With Direct Connection: In case of direct connection, the battery voltage at the end of discharge (EOD) should be no lower than the minimum VSC dc-link voltage required for reactive power delivery, i.e., $u_{b\_f} = U_{d,\min}$.

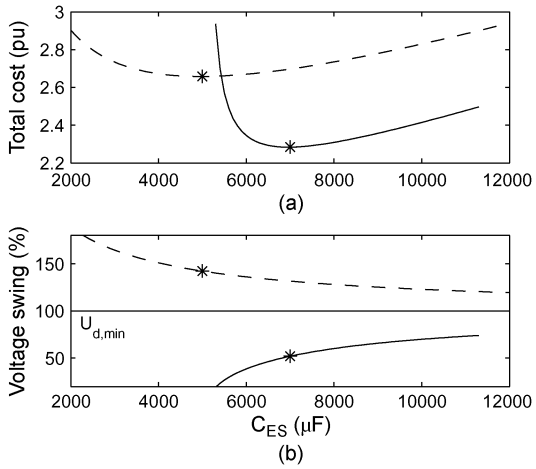

Fig. 3. Total cost and voltage swing as functions of the capacitance of the ES capacitor, with (solid) and without (dashed) interface.

The VSC rating has to be increased to

$$S_{\mathrm{Vwo}} = (1 + x\%)S_{\mathrm{base}} \tag{32}$$

and the cost of the VSC can be calculated as

$$c_{\mathrm{Vwo}} = 1 + x\%. \tag{33}$$

The total cost without interface is then obtained from (3).

IV. Cost Comparison

A. Capacitors as ES

In sizing the capacitors for ES, optimization must be performed regarding the capacitance and the voltage variation since the stored energy can be increased either by increasing the capacitance or by raising the capacitor voltage. The total cost as a function of capacitance is plotted in Fig. 3(a).

It can be seen that the optimum capacitance values are 5000μF (at a voltage level of 89 kV, corresponding to an energy level of 19.8 MJ) without interface and 7000 μF (at a voltage level of 62.6 kV, corresponding to an energy level of 13.7 MJ) with interface. The optimum designs are marked with asterisks. The total cost can be reduced from 2.66 to 2.28 p.u. with utilization of the proposed interface, corresponding to a reduction of 38% of the cost of a 100-MVA VSC. With the optimum designs, the voltage swing (relative to $U_{d,\min}$) is between 100% and 52% for the case with interface and between 100% and 142% for the case without interface, as shown in Fig. 3(b). Fig. 4 shows the accumulated cost of the different parts for the cases with and without the interface.

B. Supercapacitors as ES

The supercapacitors are supposed to deliver 20 MW for 30 s. The corresponding energy is 600 MJ.

As can be seen from Fig. 5, the optimum design without the interface is obtained with supercapacitor banks of 0.23 F and a voltage level of 110 kV (57% higher than $U_{d,\min}$). With the interface, the optimum capacitance is 0.4288 F with a voltage

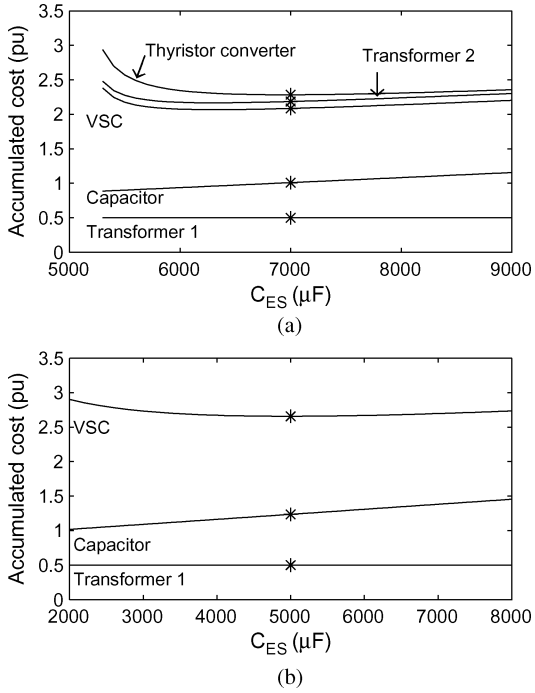

Fig. 4. Accumulated cost with capacitors as the ES. (a) With the interface. (b) Without the interface.

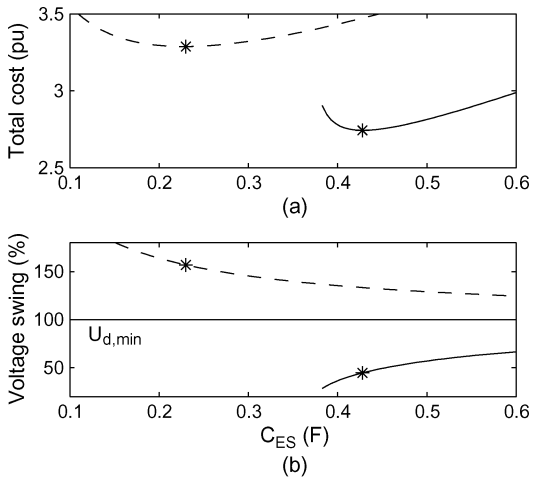

Fig. 5. Total cost and voltage swing as functions of the capacitance of the ES supercapacitor, with (solid) and without (dashed) interface.

level equal to $U_{d,\min}$. The voltage drops to 45% of $U_{d,\min}$ at the end of the energy delivery period. The power losses in supercapacitors are depicted in Fig. 6, which shows higher losses with the thyristor converter interface. The total cost can be reduced from 3.29 to 2.74 p.u. with utilization of the thyristor converter interface. The accumulated cost of different parts is plotted in Fig. 7.

C. Batteries as ES

In order to plot the cost as a function of battery voltage swing $x\%$, the quantity $y\%$ has to be determined. As listed in Table IV, the difference between $x\%$ and $y\%$ does not vary very much for different batteries. It is in the range of 12% to 20%. Thus, by

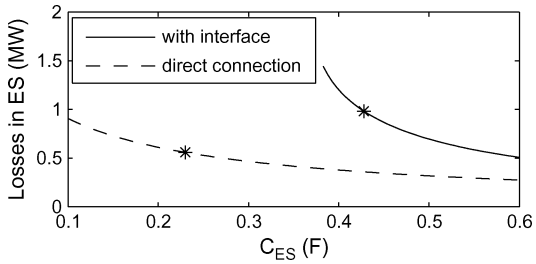

Fig. 6. Losses in the supercapacitor.

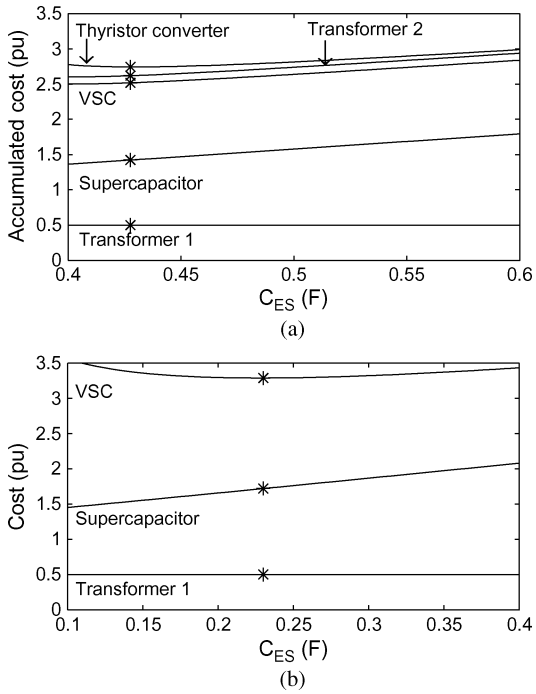

Fig. 7. Accumulated cost with the supercapacitors as ES. (a) With the interface. (b) Without the interface.

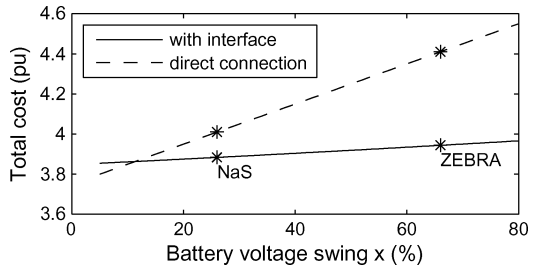

Fig. 8. Total cost as a function of battery voltage swing.

taking an intermediate value of 16%, $y\%$ can be approximated as $y\% = x\% - 16\%$.

The cost as a function of battery voltage swing $x\%$ is plotted in Fig. 8 for both cases with and without interface.

The figure shows that when the voltage swing gets beyond 12%, the total cost can be reduced by utilization of the proposed converter interface. The cost saving increases with the increase of the voltage swings. In case of NaS batteries that have a voltage swing of approximately 26%, the cost saving is 0.13 p.u. (4.01 p.u. versus 3.88 p.u.). For ZEBRA batteries, the voltage swing is as high as 66% and the cost can be reduced from 4.41 to 3.94 p.u.

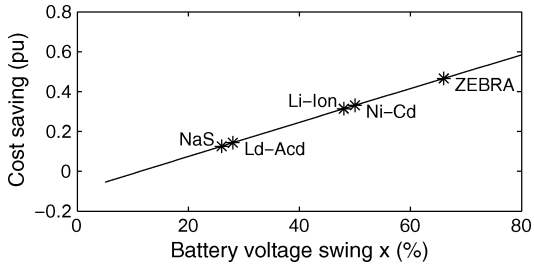

Fig. 9. Cost saving versus battery voltage swing.

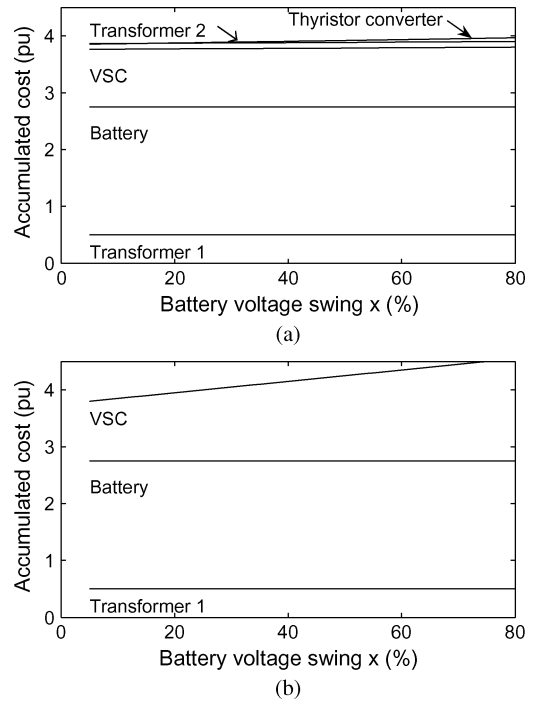

Fig. 10. Accumulated cost with batteries as ES. (a) With the interface. (b) Without the interface.

Since the battery cost is common to both cases, a clear picture of the cost saving (as a result of utilization of the proposed interface topology) as a function of battery voltage swing can be obtained regardless of the cost of batteries. This cost saving curve is depicted in Fig. 9.

The accumulated cost depicted in Fig. 10 shows that the battery cost becomes more dominating in the total cost for larger amounts of energy delivery. Therefore, the cost is the main hurdle to the application of costly batteries in large scales.

V. Cost Comparison With Capacitors, Supercapacitors, and Batteries in One Time Frame

This section presents a cost comparison for different types of ES with the same varying active power delivery period. For each active power delivery period, an optimization is made for capacitor and supercapacitor ES for both cases with and without the thyristor converter interface following the procedure described in Section III.

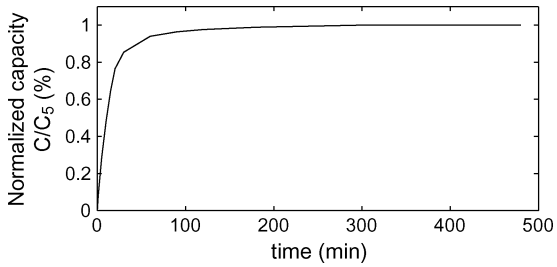

Fig. 11. Normalized capacity of SAFT Ni-Cd SBH 920 batteries versus the discharging period.

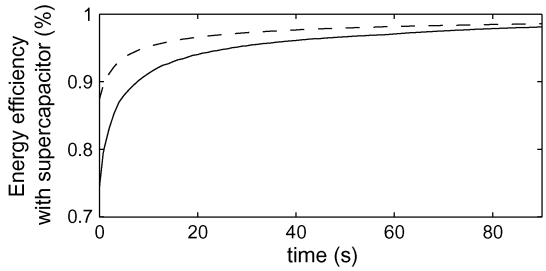

Fig. 12. Energy efficiency versus the power delivery period: with the interface (solid) and without the interface (dashed).

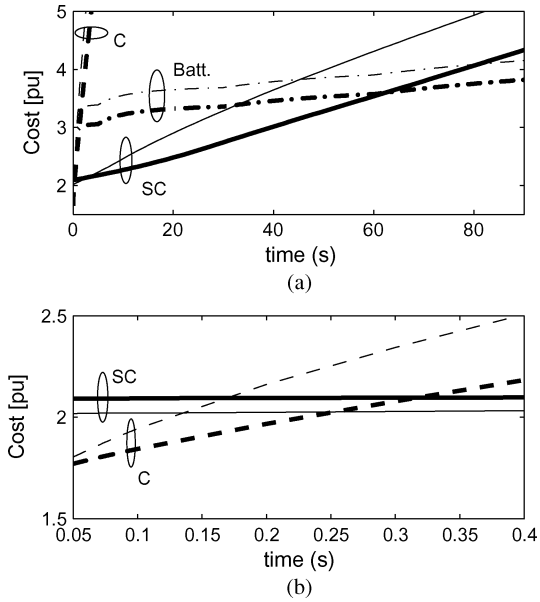

Fig. 13. Estimated cost for various power delivery periods: cost with interface (bold), cost with direct connection (normal), cost with capacitor (dashed), cost with supercapacitor (solid), and cost with battery (dash-dot).

One factor that has to be taken into consideration in making this comparison is that the capacity of batteries reduces with the increase of the discharging speed. Batteries are usually designed for long-period power delivery. The nominal capacity of batteries is usually defined as the available ampere-hours (Ah) at 5-h discharge to a certain end voltage. However, the capacity will reduce significantly if the batteries are discharged quickly. As an example, Fig. 11 shows the normalized capacity of a Ni-Cd battery as a function of discharging periods [13]. The Ni-Cd battery is used as an example since it is one of the battery types that has a field-proven record [33]. The capacities corresponding to different discharging periods are normalized with respect to the nominal capacity as defined before. It can be seen that the capacity reduces dramatically at discharges shorter than 25 min. In the following comparisons, the capacity reduction of batteries will be taken into account. The voltage swing is assumed to be 50%.

Another factor to be considered is the energy efficiency with supercapacitors. Fig. 12 depicts the energy efficiency as a function of the active power delivery period for the optimum cases. The efficiencies are calculated as the ratio of the delivered power to the sum of the delivered power and the losses in supercapacitors. It can be seen that in order to reach a reasonable efficiency (e.g., 95%), the power delivery period should be longer than 27 s with the interface and 10 s without the interface.

In the following comparisons, the cost with supercapacitors as the ES is estimated with an energy efficiency of 95%. Since the efficiency increases with the increase of the size of supercapacitors, the total cost might increase as a result. Therefore, with the limitation on the energy efficiency, the solutions with supercapacitors might not be the cost-optimized cases.

The estimated costs for the two cases with three different ES types are depicted in Fig. 13(a) for periods ranging from 0.1 s to 1.5 min., and in Fig. 13(b) from 0.05 to 0.4 s.

Due to the low cost per energy unit of battery ES, the solution with batteries becomes cheaper than with supercapacitors for power delivery periods longer than 63 s with the interface and 45 s without the interface. The solution with capacitors is cheaper than that with supercapacitors only when the energy delivery period is shorter than 317 ms with the interface and 136 ms without the interface. If the requirement on the energy efficiency becomes stricter (e.g., 98%), these two intersections will be pushed rightward to 1 s and 500 ms, respectively.

As can be observed from the two lines for supercapacitor costs in Fig. 13, the solution with the interface is not always cheaper than without the interface. The reason is that the cost is estimated with an efficiency of 95% rather than for the cost-optimized case with lower efficiency. The intersection of these two lines is 3 s.

In this comparison, the lifetime of the ES and the losses in the ES have not been taken into account. Of the three types of ES, batteries have the shortest life time in terms of the maximum number of charging-discharging cycles. Depending on the pattern of the active power delivery (occasionally or frequently), the choice of the type of ES should also take these factors into consideration. For instance, with optimum cases, the losses in supercapacitors become higher with the decrease of the discharging period. A tradeoff must be made between the initial cost and the power loss afterwards. If a loss penalty and the cost for cooling are added to the total cost, the intersection in Fig. 13(b) would be pushed considerably rightward. Capacitors have the lowest losses and the least demand on maintenance. For frequent active power deliveries with a very short period, the solution with capacitors might be the most attractive one.

VI. Conclusion

The integration of ES into a VSC involves the connection of the ES on the dc side of the VSC. Charging and discharging

processes of ES devices cause considerable voltage swings. As a result, the VSC rating has to be increased if the ES devices are connected directly to the dc link. The study shows that the total cost can be reduced by introducing the proposed dual thyristor converter as the interface between the ES and the dc link of the VSC. The cost comparison between different types of ES, even considering the rough simplification and the uncertainty of cost figures, provides a guideline for the choice of ES when several alternatives exist.

REFERENCES

[1] Z. Yang, C. Shen, L. Zhang, M. Crow, and S. Atcitty, "Integration of a StatCom and battery energy storage," *IEEE Trans. Power Syst.*, vol. 16, no. 2, pp. 254–260, May 2001.

[2] K. Kobayashi, M. Goto, K. Wu, Y. Yokomizu, and T. Matsumura, "Power system stability improvement by energy storage type STATCOM," presented at the IEEE Power Tech Conf., Bologna, Italy, 2003.

[3] A. Arulampalam, J. Ekanayake, and N. Jenkins, "Application study of a STATCOM with energy storage," *Proc. Inst. Elect. Eng., Gen., Transm., Distrib.*, vol. 150, pp. 373–384, May 2003.

[4] A. Arsoy, Y. Liu, S. Chen, Z. Yang, M. Crow, and P. Ribeiro, "Dynamic performance of a static synchronous compensator with energy storage," in *Proc. IEEE Power Eng. Soc. Winter Meeting*, 2001, pp. 605–610.

[5] Y. Cheng, C. Qian, M. L. Crow, S. Pekarek, and S. Atcitty, "A comparison of diode-clamped and cascaded multilevel converters for a STATCOM with energy storage," *IEEE Trans. Ind. Electron.*, vol. 53, no. 5, pp. 1512–1521, Oct. 2006.

[6] A. Arulampalam, M. Barnes, N. Jenkins, and J. Ekanayake, "Power quality and stability improvement of a wind farm using STATCOM sup-ported with hybrid battery energy storage," *Proc. Inst. Elect. Eng., Gen., Transm., Distrib.*, vol. 153, pp. 701–710, Nov. 2006.

[7] C. Banos, M. Aten, P. Cartwright, and T. Green, "Benefits and control of STATCOM with energy storage in wind power generation," in *Proc. 8th Inst. Elect. Eng. Int. Conf. AC and DC Power Transmission*, 2006, pp. 230–235.

[8] P. Srithorn, M. Sumner, L. Yao, and R. Parashar, "The control of a STATCOM with supercapacitor energy storage for improved power quality," in *Proc. CIRED Seminar: Smart Grids for Distribution*, 2008.

[9] M. Steurer and S. Eckroad, "Voltage control performance enhancement by adding energy storage to shunt connected voltage source converters," in *Proc. 10th Int. Conf. Harmonics Quality Power*, 2002, pp. 590–594.

[10] H. Wrede and V. Staudt, "Optimized feed forward control of a STATCOM with limited energy storage capability for flicker compensation," in *Proc. IEEE 35th Annu. Power Electron. Specialists Conf.*, 2004, pp. 3157–3163.

[11] Z. Xi, B. Parkhideh, and S. Bhattacharya, "Improving distribution system performance with integrated STATCOM and supercapacitor energy storage system," in *Proc. IEEE Power Electron. Specialists Conf.*, 2008, pp. 1390–1395.

[12] H. Xie, L. Ängquist, and H. P. Nee, "Investigation of StatComs with capacitive energy storage for reduction of voltage phase jumps in weak networks," *IEEE Trans. Power Syst.*, vol. 24, no. 1, pp. 217–225, Feb. 2009.

[13] SAFT Ni-Cd SBH Battery Datasheet. [Online]. Available: http://www.saftbatteries.com/doc/Documents/stationary/Cube782/bbdatacom_en_0407.82a9e3d8-da51-4d80-8e0c-83faef0c0391.pdf p. 26

[14] G. Ariyoshi, K. Harada, K. Yamasaki, and K. Murata, "Load leveling using EDLCs under PLL control," in *Proc. 15th Annu. IEEE Appl. Power Electron. Conf. Expo.*, 2000, pp. 774–780.

[15] A. Kotsopoulos, J. Duarte, and M. Hendrix, "A converter to interface ultra-capacitor energy storage to a fuel cell system," in *Proc. IEEE Int. Symp. Ind. Electron.*, 2004, pp. 827–832.

[16] S. Ponnaluri, G. O. Linhofer, J. K. Steinke, and P. K. Steimer, "Comparison of single and two stage topologies for interface of BESS or fuel cell system using the ABB standard power electronics building blocks," presented at the Eur. Conf. Power Electron. Appl., Dresden, Germany, 2005.

[17] S.-M. Kim and S.-K. Sul, "Control of rubber tyred gantry crane with energy storage based on supercapacitor bank," *IEEE Trans. Power Electron.*, vol. 21, no. 5, pp. 1420–1427, Sep. 2006.

[18] Y. Hu, J. Tatler, and Z. Chen, "A bidirectional DC/DC power electronic converter for an energy storage device in an autonomous power system," in *Proc. 4th Int. Power Electron. Mot. Control Conf.*, 2004, pp. 171–176.

[19] T. Mishima and E. Hiraki, "ZVS-SR bidirectional DC-DC converter for supercapacitor-applied automotive electric energy storage systems," presented at the IEEE Vehicle Power and Propulsion Conf., Chicago, IL, 2005.

[20] M. Ortuzar, J. Moreno, and J. Dixon, "Ultracapacitor-based auxiliary energy system for an electric vehicle: Implementation and evaluation," *IEEE Trans. Ind. Electron.*, vol. 54, no. 4, pp. 2147–2156, Aug. 2007.

[21] J. Moreno, M. Ortuzar, and J. Dixon, "Energy-management system for a hybrid electric vehicle, using ultracapacitors and neural networks," *IEEE Trans. Ind. Electron.*, vol. 53, no. 2, pp. 614–623, Apr. 2006.

[22] H. Tao, J. Duarte, and M. Hendrix, "Line-interactive UPS using a fuel cell as the primary source," *IEEE Trans. Ind. Electron.*, vol. 55, no. 8, pp. 3012–3021, Aug. 2008.

[23] H. Xie, L. Ängquist, and H. P. Nee, "A converter topology suitable for interfacing energy storage with the dc link of a StatCom," presented at the Ind. Appl. Soc. Annu. Meeting, Edmonton, AB, Canada, 2008.

[24] H. Xie, L. Ängquist, and H. P. Nee, "Design and analysis of a controller for a converter interface interconnecting an energy storage with the Dc link of a VSC," *IEEE Trans. Power Syst.*, vol. 25, no. 2, pp. 1007–1015, May 2010.

[25] J. A. Kosek, B. M. Dweik, and A. B. LaConti, *Technical Characteristics of PEM Electrochemical Capacitors. Handbook of Fuel Cells*. Hoboken, NJ: Wiley, 2003, ch. 50, pp. 747–760.

[26] A. Burke, "Ultracapacitor technologies and application in hybrid and electric vehicles," *Int. J. Energy Res.*, vol. 34, pp. 131–151, 2010.

[27] Nesscap Catalogue 2011: Power to Move You to Next. [Online]. Available: http://www.nesscap.com/images/news/Nesscapcatalogue_2011.pdf

[28] NESSCAP ultracapacitor datasheet. 2011. [Online]. Available: http://www.nesscap.com/product/edlc_large1.jsp

[29] J. L. Sudworth, "The sodium/nickel chloride (ZEBRA) battery," *J. Power Sources*, vol. 100, no. 1–2, p. 149, 2001.

[30] L. W. Chung, M. Siam, A. Ismail, and Z. Hussien, "Modeling and simulation of sodium sulfur battery for battery-energy storage system and custom power devices," presented at the Nat. Power Energy Conf., Kuala Lumpur, Malaysia, 2004.

[31] I. Papic, "Simulation model for discharging a lead-acid battery energy stor-age system for load leveling," *IEEE Trans. Energy Convers.*, vol. 21, no. 2, pp. 608–615, Jun. 2006.

[32] L. Gao, S. Liu, and R. Dougal, "Dynamic lithium-ion battery model for system simulation," *IEEE Trans. Compon. Packag. Technol.*, vol. 25, no. 3, pp. 495–505, Sep. 2002.

[33] J. McDowall, "High power batteries for utilities—The world's most powerful battery and other developments," in *Proc. IEEE Power Eng. Soc. Gen. Meeting*, 2004, pp. 2034–2037.

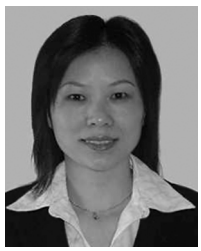

Hailian Xie was born in Henan, China, in 1969. She received the M.Sc. and Ph.D. degrees from the Royal Institute of Technology (KTH), Stockholm, Sweden, in 2004 and 2009, respectively.

Currently, she is with ABB (China) Ltd., Corporate Research, Beijing, China. Her research interests are the control of flexible ac transmission systems devices and HVDC, power-electronics converters, energy storage, and grid integration of wind power.

Lennart Ängquist (M'05) was born in Växjö, Sweden, in 1946. He received the M.Sc. degree from Lund Institute of Technology, Lund, Sweden, in 1968 and the Ph.D. degree from Royal Institute of Technology, Stockholm, in 2002.

Currently, he is with ABB (formerly ASEA), involved in various technical departments. He worked on industrial and traction motor drives from 1974 to 1987. After that, he worked on flexible ac transmission system applications in electrical power systems. He is an Adjunct Professor at the Royal Institute of Technology.

Hans-Peter Nee (S'91–M'96–SM'04) was born in Västerås, Sweden, in 1963. He received the M.Sc., Licentiate, and Ph.D. degrees in electrical engineering from the Royal Institute of Technology, Stockholm, Sweden, in 1987, 1992, and 1996, respectively.

He was appointed Professor of Power Electronics in the Department of Electrical Engineering, Royal Institute of Technology, in 1999. His interests are power-electronic converters, semiconductor components, and control aspects of utility applications, such as flexible ac transmission systems and HVDC as well as variable-speed drives.

Prof. Nee received the Energy Prize from the Swedish State Power Board in 1991, the ICEM'94 (Paris) Verbal Prize in 1994, the Torsten Lindström Electric Power Scholarship in 1996, and the Elforsk Scholarship in 1997. He has served the board of the IEEE Sweden Section for many years and was the Chairman of the board during 2002 and 2003. He is also a member of EPE and serves the Executive Council and the International Steering Committee. He is also active in the IEC and the corresponding Swedish organization SEK in the committees TC 25 and TK 25, respectively.